Dobson, D. P., Hunt, S. A., McCormack, R., Lord, O. T., Donald J., W., Li, L., & Walker, A. M. (2010). Thermal diffusivity of MORB-composition rocks to 15 GPa: implications for triggering of deep seismicity. *High Pressure Research*, *30*(3), 406-414. https://doi.org/10.1080/08957959.2010.516827

Thermal diffusivity of MORB-composition rocks to 15 GPa; implications for triggering of deep seismicity.

David P. Dobson[1], Simon A. Hunt[1,3], Richard McCormack[1], Oliver T. Lord[2], Donald J. Weidner[3], Li Li[3] and Andrew M. Walker[1,2].

1. Department of Earth Sciences, University College London.
2. Department of Earth Sciences, University of Bristol.
3. Mineral Physics Institute, State University New York at Stony Brook.

Received:
Accepted:

Short title: Thermal diffusivity of MORB

Thermal diffusivity of MORB-composition rocks to 15 GPa; implications for triggering of deep seismicity.

David P. Dobson[1], Simon A. Hunt[1], Richard McCormack[1], Oliver T. Lord[2], Donald J. Weidner[3], Li Li[3] and Andrew M. Walker[1].

1. Department of Earth Sciences, University College London.
2. Department of Earth Sciences, University of Bristol.
3. Mineral Physics Institute, State University New York at Stony Brook.

Abstract

We have measured the thermal diffusivity of eclogite and majorite with a model MORB composition at pressures of 3 and 15 GPa respectively. Both phase assemblages show inverse dependences of their thermal diffusivities on temperature: $D_{eclogite}=9(10)\times10^{-10}+7(1)\times10^{-4}/T(K)$ m^2/s and $D_{majorite}=6.2(5)\times10^{-7}+3.0(5)\times10^{-4}/T(K)$ m^2/s. The values for majorite are in good agreement with previous measurements for other garnets and are considerably lower than thermal diffusivities of wadsleyite and ringwoodite which are the main components of the mantle transition zone. We discuss the implications of the low thermal conductivity of subducted oceanic crust in the transition zone for the triggering of deep seismicity.

Introduction

Conductive heat transport through mantle materials plays a fundamental role in mantle convection and hence the secular cooling of the Earth. It is the main mechanism for thermally equilibrating subducting oceanic lithosphere with the surrounding mantle which, in turn, determines the depth of the equilibrium (and metastable) phase transitions and buoyancy forces in subducting slabs. However, despite their importance for mantle dynamics, the thermal conductivity, κ, and diffusivity, D, of mantle minerals at high pressure are very poorly constrained. For example, there are no measurements for perovskite above 1 atmosphere and 340 K (Osako and Ito, 1991) and only one set of thermal diffusivity measurements of the high-pressure polymorphs of Mg_2SiO_4, wadsleyite and ringwoodite (Xu et al., 2004).

The case for garnet is hardly better with measurements on a range of garnet compositions at atmospheric pressure (Kanamori et al., 1968; Horai, 1971; Osako, 1997; Hofmeister, 2006, Marquidt et al., 2009) and one high-pressure (8GPa) measurement for an almandine-rich garnet (Osako et al., 2004); no measurements have been performed on majorite garnet which, in the mid-transition zone, constitutes almost the entirety of the crustal portion of the subducting slab. Here we present measurements of thermal diffusivity of a model MORB composition at 3 and 15 GPa where the stable phase assemblages are eclogite (containing pyrope-rich garnet and omphacite) and pure majorite, respectively.

Methods

Principle

Thermal diffusivity was measured using the modified Ångstrom method described previously (Dobson et al., 2008). In the high-pressure implementation of the Ångstrom method a stationary thermal wave is developed in a sample by perturbing the temperature in the surrounding cylindrical furnace in a manner which varies sinusoidally with time. As long as the sample is sufficiently long for the infinite cylinder approximation to be valid (sample length $\geq$ 1.5 times the diameter) the phase lag, Φ_0-Φ_R, and amplitude difference, θ_0/θ_R, of the thermal wave between points at the axis of the sample and radius, R, are related to the thermal diffusivity by (Khedari *et al*., 1995):

$$\Phi = \Phi_0 - \Phi_R = \tan^{-1}\left(\frac{bei(A)}{ber(A)}\right) \quad (1a),$$

$$\theta = \frac{\theta_0}{\theta_R} = \frac{1}{\sqrt{ber^2(A) + bei^2(A))}} \quad (1b)$$

and

$$A = \left(\frac{\omega R^2}{\kappa}\right)^{1/2} \quad (1c),$$

where *ber* and *bei* are Kelvin functions of the zero order Bessel functions (e.g.; Brualla and Martin, 2001), and ω is the angular frequency of the temperature perturbation. In practice the phase lag is considered to give a more accurate measure of the thermal diffusivity (Katsura, 1993; Khedari et al., 1995; Xu et al., 2004) and the phase lag was used here rather than the amplitude difference.

Ordinarily the phase lag is determined by inserting two thermocouples, one along the sample axis and the other at the outside edge of the sample; this is extremely non-trivial at high pressure (e.g. Katsura, 1993) and has proven to be a limiting problem for measuring the thermal diffusivity of magnesium silicate perovskite. Furthermore, there are problems associated with the temperature measurement technique: the thermal mass of the thermocouple might perturb the temperature field in the sample and there might be imperfect thermal contact between the thermocouple and the sample (for example, Hofmeister [2007] suggests that multiple contact methods might be inaccurate by up to 30%). Here we measure the thermally induced change in length of the sample as a *proxy* for the temperature change, using synchrotron radiography (Dobson et al., 2008). For a given change in temperature, ΔT, the change in length of the sample, Δl is given by the thermal expansivity: $\Delta l = l\alpha\, \Delta T$, where l is the sample length at T and α is the linear thermal expansivity. Assuming (i) that the thermal expansivity is constant across the temperature range of the imposed thermal wave (small ΔT and/or temperature above the Debye temperature) and (ii) the thermo-elastic strain is instantaneous on a change in temperature (no plastic deformation) then the change in length of the sample can be used

directly in equations (1) without converting it to the temperature. The precision in fitting the sine wave is then a function in precision of length measurement. Both of these assumptions are valid for the magnitude of temperature perturbation used here. Thin strips of X-ray absorbing foils are placed radially at the end of the sample, perpendicular to the incident X-ray beam, such that radiographic images of the foils define the length of the sample at all radii. This has several advantages over two-thermocouple methods: (i) the sample geometry is simplified, requiring discs of high-pressure sample; (ii) the phase lag can be determined at all radii over which the sample is imaged; (iii) the observation of thermal expansion along the sample averages the temperature field along the length of the sample between the marker foils, minimising effects of local temperature perturbations around the foils; and (iv) since the thermal expansion of the sample is observed, contact problems are removed. These last two advances solve the problems previously associated with the Ångstrom method and discussed in a recent review of thermal transport measurements (Hofmeister, 2007).

Experiments

Figure 1 shows a schematic drawing of the high-pressure cell. Samples were placed at the centre of an octahedral high-pressure cell, directly inside graphite furnaces for radiographic measurements. Marker foils were placed ~2 mm apart along the length of the samples. NaCl powder was packed at the end of the samples to fill up the remainder of the furnace. Radiographic images were collected using white X-rays exciting a 200 μm thick YAG crystal; the optical fluorescence from the crystal was imaged using a 'Prosilica' optical CCD camera with telephoto lens such that each pixel imaged 2 μm x 2 μm of the sample. Cross-correlation between successive images and cross-convolution of the top and bottom foil allows the length change of the samples to be determined with a precision of ~0.1 pixel at any arbitrary radius.

Experiments were performed using a 200 Ton 6/8 multi-anvil press installed at beamline X17B2 of the National Synchrotron Light Source. MgO cells of 8, or 7, mm edge length were compressed using hard anvils with 3 mm truncations; the 4 anvils in the X-ray beam were made of cubic boron nitride and the 4 anvils not in the beam were tungsten carbide. Thermal diffusion measurements were performed at 3.5, or 15, GPa for eclogite and

majorite respectively. Experiments were performed by compressing the sample at room temperature to the target pressure, followed by step-wise heating. The sample was left to thermally equilibrate for ~5 minutes at each temperature before starting the temperature perturbation for thermal diffusion measurements: the temperature was controlled using a thermocouple placed just outside the furnace, as indicated in Figure 1. Temperature perturbations were generated by putting a sinusoidal perturbation on the control *current* of the furnace; deviations from sinusoidal *temperature* variation were sufficiently small that a sinusoidal fit to the observed thermal expansion was perfectly adequate (Figure 2). Perturbations of ± 30-50 K at the furnace were used in the present study, corresponding to maximum thermal strains of ~0.4 μm in the sample. Sine waves with periods of 0.5, 1, 2, 4 and 8 s were used for the temperature control. The temperature cycle was started ~1 minute before starting the radiographic observations to ensure steady state had been attained in the sample; 10 frames were collected per cycle for 100 cycles of the temperature wave (1000 frames in total). For full details of the method see Dobson et al., 2008 and Li et al., 2003.

Samples

Samples of eclogite and majorite were synthesised from a synthetic glass with a composition similar to the primitive abyssal tholeite ARP74 (Table 1) which transforms to pure majorite (Nishihara, 2005); glass was synthesised by fusion in air of a mixture of oxides (Fe, Mn, Mg, Si, Ti, Al), carbonates (Ca, Na, K) and $Ca_3(PO_4)_2$. This mixture was decarbonated and fused in a platinum crucible, which had been pre-saturated with iron, and quenched into water. Two cycles of grinding and glassing ensured compositional homogeneity, after which the glass was reduced in Ar-H mixture at 1073 K for 20 h.

Eclogite samples were synthesised from the MORB glass at 3 GPa and 1473 K for 24h in a 1000 tonne 6/8 multi anvil press installed at UCL. Majorite was synthesised from the glass at 15GPa and 1973 K for 4 h using the 5000 tonne press at the Bayerisches Geoinstitut. Recovered samples were analysed by X-ray diffraction to confirm phase purity and then cored into cylinders with a diameter of 2 mm for radiographic measurements. The transformed samples, prior to the thermal diffusion measurement, were polycrystalline and homogeneous, with grain size of around ten microns. This

ensured that radiative conduction was not significant except at the highest temperatures (e.g.; Hofmeister et al., 2007)

Results

Eclogite

An example of the observed thermal expansion at three arbitrary radii is shown for the eclogite sample at 976 K and 0.5 Hz driving wave in Figure 2; this figure is typical of the observed thermal expansion waves for all of the data collected in this study. The observed amplitude of the thermal strain at the edge of the sample is approximately half that predicted from the thermal expansivity of the sample. This reduced amplitude is probably due to (1) the fact increasing temperature also causes an increase in sample pressure; the relative strengths of the thermally induced stress and strain being a complex function of the lengths, and relative thermoelastic properties of the sample and surrounding pressure medium as well as the temperature profile along the entire furnace, and (2) self-constriction within the sample by regions with different thermal strains. This convolution effect on the thermal strain further mitigates against the use of amplitude for determining thermal diffusivity (eq. 1b) in the present experiments. However, as long as the thermoelastic strains are instantaneous the phase lag is not affected by the thermal stresses imposed on the sample by the surrounding pressure medium, making the use of equation 1a robust even under these complex conditions.

The variation of phase with radius for eclogite at 680 K and 1 Hz driving frequency is shown in Figure 3. The fit of equation 1 to the data is also plotted; in practice a global non-linear least-squares routine was used to fit equation 1 to all radii and periods simultaneously. The thermal diffusivity of MORB-composition eclogite is plotted against temperature in Figure 4. We have chosen to fit the data to two commonly used diffusivity-temperature relationships; D=a+b/T (e.g.; Osako et al., 2004) and $1/D$=a+bT+cT^2… (e.g.; Hoffmeister 2007). The fitting parameters are: D=9(10)x10^{-10}+7(1)x10^{-4}/T(K) m^2/s, and $1/D$=8x10^5-1.1x10^3T+1.9T^2 s/m^2; both are equally good for this sparse dataset.

Majorite

The thermal diffusivity of MORB composition majorite at 15 GPa is plotted against temperature in Figure 5, along with previous measurements for similar garnets. Weighted least-squares regressions to the majorite data yield the equations D=6.2(5)x10^{-7}+ 3.0(5)x10^{-4}/T (K) m^2/s and $1/D$=2.26x10^5+1.57*10^3T-0.85748T^2+1.52x$10^{-04}T^3$ s/m^2; both fits are essentially identical in the fitted temperature range. The two highest-temperature data deviate significantly from the fitted curve; this is likely to be due to a significant radiative component to the thermal conduction at these temperatures. These two points were therefore not included in the regressions.

Comparison with previous results

There are no previous measurements of thermal diffusivity in highly majoritic garnets for direct comparison with the present results. We have therefore plotted on figure 5 previously measured thermal diffusivity of a 73% almandine, 25% pyrope garnet at atmospheric pressure and 8 GPa from Osako *et al*. (2004) and a 75% pyrope 15% almandine 12% grossular garnet at atmospheric pressure (Hoffmeister, 2006), which are the closest compositions available in the literature. Despite the differences in composition (the present garnet is approximately 33% grossular, 20% almandine, 16% pyrope and 13% majorite) the temperature dependences are similar and there is an approximately constant positive dependence of thermal diffusivity on pressure. By 15 GPa the present measurements are approximately 1.5 times higher than the atmospheric pressure values. This is consistent with the predicted pressure dependence of thermal diffusivity of Hofmeister (2007). Furthermore, a recent study (Marquardt *et al*., 2009) surveyed the thermal diffusivities of a wide range of natural and synthetic garnets at atmospheric pressure and concluded that, in the high-temperature limit, they all had the same value of thermal diffusivity, D_{min}, of 6.4(3) x 10^{-7} m^2/s. This compares very well with the present high-temperature limit value of 6.2(5) x 10^{-7} m^2/s and gives us confidence that the present results for MORB composition majorite at 15 GPa are robust. The present measurements are similarly consistent with the calculations of Geisting *et al*. (2004) for an appropriate garnet composition.

Discussion

The present results have some implications for the thermal reequilibration of subducted slabs. Figure 6 shows the thermal diffusivity of MORB composition majorite and eclogite, along with the polymorphs of Mg_2SiO_4 (from Xu *et al*., 2004), plotted as a function of temperature. The thermal diffusivities of the MORB assemblages measured here are similar to that of olivine and 30-40% smaller than that of wadsleyite and ringwoodite at 1000 K. Thermal models of subducting slabs which use the thermal conductivities of the appropriate mineral assemblage (Marton *et al*., 2005) show that the extent of metastable olivine is reduced compared to earlier thermal models which just used olivine thermal conductivities. The present results, which show that the thermal diffusivity (and hence thermal conductivity) of majorite is similar to that of olivine would suggest that the MORB layer on the top of the subducting slab would have an anomalously low thermal conductivity, compared to the surrounding wadsleyite- and ringwoodite-rich assemblages, in the transition zone. This MORB layer is thin compared with the rest of the subducting slab and so its effect on slab thermal equilibration at long timescales is likely to be small. At short timescales, however, where the lengthscale of a thermal transient is shorter than a few kilometers the reduced thermal conductivity of the oceanic crustal layer might be significant.

It has been suggested that deep earthquakes within the transition zone are triggered by thermal run-away processes on shear zones of a few tens of meters in thickness (Griggs and Baker, 1969; Ogawa, 1987; Karato et al., 2001). Thermal run away is consistent with the low rupture velocities and low seismic efficiencies of many transition-zone depth earthquakes (e.g.; Wiens, 2001). The efficiency of thermal run-away is inversely proportional to the thermal conductivity of the shearing medium. The current results suggest, therefore that thermal run-away leading to triggering of deep seismicity in the transition zone should be more likely in the majorite-rich crustal portion of the subducting slab. The stability field of majoritic garnet corresponds well with the depth range over which there is a peak in deep earthquake activity (~500-600 km). Furthermore, seismicity in the Tonga slab at these depths appears to be primarily located

within the upper ~10 km of the slab (eg Estabrook, 2004), implicating majorite in the triggering mechanism.

Summary and conclusions.

We have measured the thermal diffusivity of the 'ecolgitic' and 'majoritic' phase assemblages of a model MORB composition at pressures and temperatures appropriate to subducting oceanic crust. Increasing pressure results in two competing effects on MORB thermal diffusivity: (i) for a given phase assemblage, the effect of pressure is to increase its thermal diffusivity. (ii) The garnet content of the equilibrium phase assemblage increases with pressure until, at around 15 GPa, MORB is almost pure garnet. Since garnet has a low thermal conductivity compared to other mantle silicate minerals these two effects tend to cancel out such that there is very little difference in thermal conductivity at 3 GPa and 15 GPa in the MORB composition studied here. This is very different from the main component of mantle peridotite, Mg_2SiO_4, which shows a factor of two increase in thermal diffusivity from 1 to 20 GPa at a given temperature. Majorite's inefficiency at transporting heat will cause subducted oceanic crust to thermally reequilibrate with the surrounding mantle more slowly than olivine-rich portions of the subducting slab; if MORB can accumulate in the transition zone, these regions might contain long-lived thermal anomalies. Furthermore, the lower thermal diffusivity of the crustal portion of the slab in the transition zone might explain the localisation of some deep earthquakes to the top of the slab if the triggering mechanism requires positive thermal-feedback processes.

Acknowledgements

We acknowledge financial support from the following sources: Marie Curie Research Training Network "c2c" Contract No. MRTN-CT-2006-035957, The Royal Society (DPD), NERC grant NE/E012922/2 (AMW); NSF grant EAR0809397 (LL). Use of the National Synchrotron Light Source, Brookhaven National Laboratory, was supported by the US Department of Energy, Office of Science, Office of Basic Energy Sciences, under Contract No. DE-AC02-98CH10886. We thank W. Crichton and two anonymous reviewers for helpful comments.

References

Brualla, L. & Martin, P., 2001. Analytic approximations to Kelvin functions with applications to electromagnetics, *J Phys a-Math Gen,* 34**,** 9153-9162.

Dobson, D.P., Hunt, S.A., Li, L. & Weidner, D., 2008. Measurement of thermal diffusivity at high pressures and temperatures using synchrotron radiography, *Mineral Mag,* 72**,** 653-658.

Estabrook, C.H., 2004. Seismic constraints on mechanisms of deep earthquake rupture, *J Geophys Res-Sol Ea,* 109**,** doi:10.1029/2003JB002449.

Giesting, P.A., Hofmeister, A.M., Wopenka, B., Gwanmesia, G.D. & Jolliff, B.L., 2004. Thermal conductivity and thermodynamics of majoritic garnets: implications for the transition zone, *Earth Planet Sc Lett,* 218**,** 45-56.

Griggs, D.T. & Baker, D.W., 1969. The origin of deep focus earthaukes. *in Properites of matter under unusual conditions*, pp. 23-42, eds. Mark H & Fernbach, S. Wiley, New York.

Hofmeister, A.M., 2006. Thermal diffusivity of garnets at high temperature, *Phys Chem Miner,* 33**,** 45-62.

Hofmeister, A.M., 2007. Properties of rocks and minerals-Thermal conductivity of the Earth. *in Treatise on Geophysics*, pp. 543-577, ed. Price, G. D. Elsevier, Amsterdam.

Horai, K.I., 1971. Thermal Conductivity of Rock-Forming Minerals, *J Geophys Res,* 76**,** 1278-1308.

Kanamori, H., Fujii, N. & Mizutani, H., 1968. Thermal Diffusivity Measurement of Rock-Forming Minerals from 300 Degrees to 1100 Degrees K, *J Geophys Res,* 73**,** 595-&.

Karato, S., Riedel, M.R. & Yuen, D.A., 2001. Rheological structure and deformation of subducted slabs in the mantle transition zone: implications for mantle circulation and deep earthquakes, *Phys Earth Planet In,* 127**,** 83-108.

Katsura, T., 1993. Thermal-Diffusivity of Silica Glass at Pressures up to 9-Gpa, *Phys Chem Miner,* 20**,** 201-208.

Khedari, J., Benigni, P., Rogez, J. & Mathieu, J.C., 1995. New Apparatus for Thermal-Diffusivity Measurements of Refractory Solid Materials by the Periodic Stationary Method, *Rev Sci Instrum,* 66**,** 193-198.

Li, L., Raterron, P., Weidner, D. & Chen, J., 2003. Olivine flow mechanisms at 8 GPa. *Phys Earth Planet In*, 138, 113–129.

Marquardt, H., Ganschow, S. & Schilling, F.R., 2009. Thermal diffusivity of natural and synthetic garnet solid solution series, *Phys Chem Miner,* 36**,** 107-118.

Marton, F.C., Shankland, T.J., Rubie, D.C. & Xu, Y.S., 2005. Effects of variable thermal conductivity on the mineralogy of subducting slabs and implications for mechanisms of deep earthquakes, *Phys Earth Planet In,* 149**,** 53-64.

Nishihara, Y., Aoki, I., Takahashi, E., Matsukage, K.N. & Funakoshi, K., 2005. Thermal equation of state of majorite with MORB composition, *Phys Earth Planet In,* 148**,** 73-84.

Ogawa, M., 1987. Shear instability in a viscoelastic material as the cause of deep focus earthquakes. , *J Geophys Res* 92**,** 13801–13810

Osako, M., 1997. , 1997. Thermal diffusivity of olivine and garnet single crystals. , *Bulletin of the National Science Museum, Tokyo,* E20**,** 1-7.

Osako, M. & Ito, E., 1991. Thermal-Diffusivity of Mgsio3 Perovskite, *Geophys Res Lett,* 18**,** 239-242.

Osako, M., Ito, E. & Yoneda, A., 2004. Simultaneous measurements of thermal conductivity and thermal diffusivity for garnet and olivine under high pressure, *Phys Earth Planet In,* 143-44**,** 311-320.

Wiens, D.A., 2001. Seismological constraints on the mechanism of deep earthquakes: temperature dependence of deep earthquake source properties. *Phys Earth Planet In,* 127, 145-163.

Xu, Y.S., Shankland, T.J., Linhardt, S., Rubie, D.C., Langenhorst, F. & Klasinski, K., 2004. Thermal diffusivity and conductivity of olivine, wadsleyite and ringwoodite to 20 GPa and 1373 K, *Phys Earth Planet In,* 143-44**,** 321-336.

Figure Captions.

Figure 1. Schematic drawing of the pressure assembly used for the radiographic measurement of thermal diffusivity. A) Cross-section of the cell containing the axis of the furnace. B) Cross section a-a' perpendicular to the furnace axis.

Figure 2. Thermal expansion curves of MORB eclogite at three arbitrary radii. The graph shows, for clarity, thermal expansions derived from all 1000 frames of the measurement, convolved onto a single temperature cycle. Each set of data has been arbitrarily offset from the amplitude origin for display purposes. The inclined solid line demonstrates the phase lag with reducing radius. The sample was at 70 tons load and 976 K mean temperature; the frequency of the driving wave was 0.5 Hz.

Figure 3. An example of the phase lag with varying radius determined from the radiography time-series.

Figure 4. The variation of thermal diffusivity of MORB composition eclogite with temperature at 3.5 GPa.

Figure 5. The variation of thermal diffusivity of garnet with temperature. The least-squares fit to the data (solid line) did not include the two highest-temperature data; see text for discussion. Squares; MORB composition majoritic garnet at 15 GPa (the solid line is the fit to the data): Circles and dotted line; almandine-pyrope garnet at 8 GPa (from Osako et al., 2004): dot-dashed lines; almandine-pyrope at atmospheric pressure. The faint dot-dashed line is for the same composition as the 8 GPa data (Osako, 1997), the bold line is for a more pyrope-rich composition which should be more comparable to the present results ('Xenolith' sample of Hoffmeister, 2006).

Figure 6. Thermal diffusivity of eclogite and majorite (this study), and olivine, wadsleyite and ringwoodite (Xu et al., 2004) as a function of temperature. Majorite and eclogite have thermal diffusivities which are similar to olivine and 1.5-2 times smaller than ringwoodite and wadsleyite.

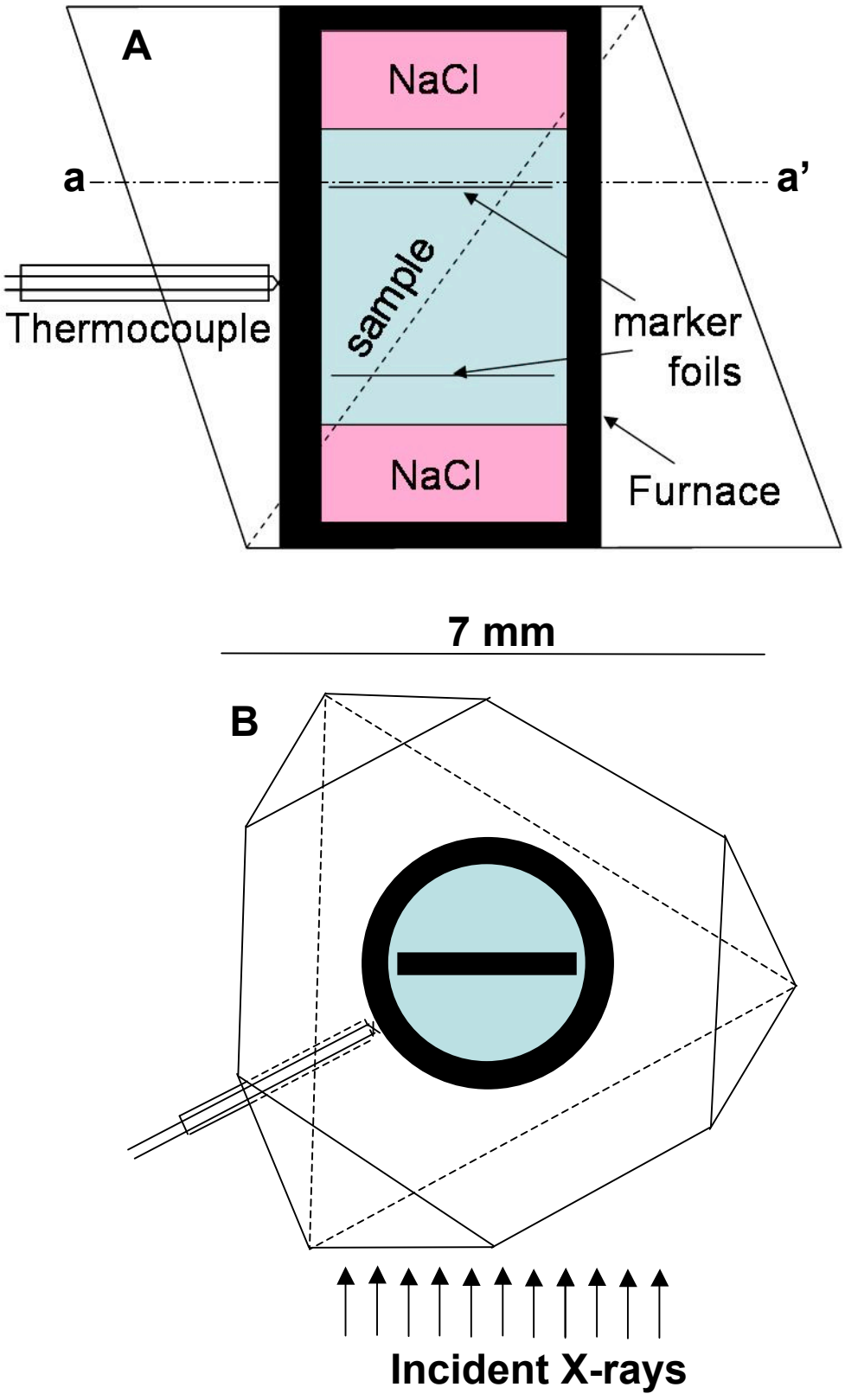
A
NaCl
a
a'
sample
Thermocouple
marker
foils
NaCl
Furnace
7 mm
B
Incident X-rays

Figure 1.

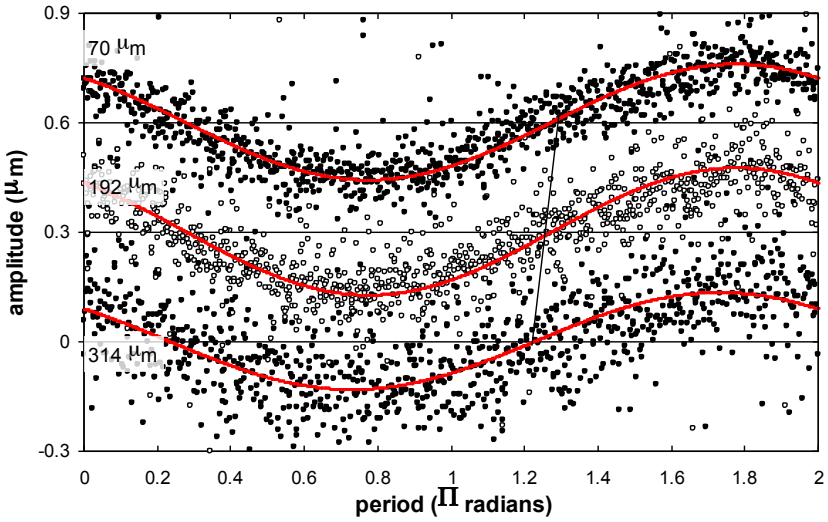
0.9
0.6
0.3
0
-0.3
amplitude (μm)
70 μm
192 μm
314 μm
0
0.2
0.4
0.6
0.8
1
1.2
1.4
1.6
1.8
2
period (Π radians)

Figure 2.

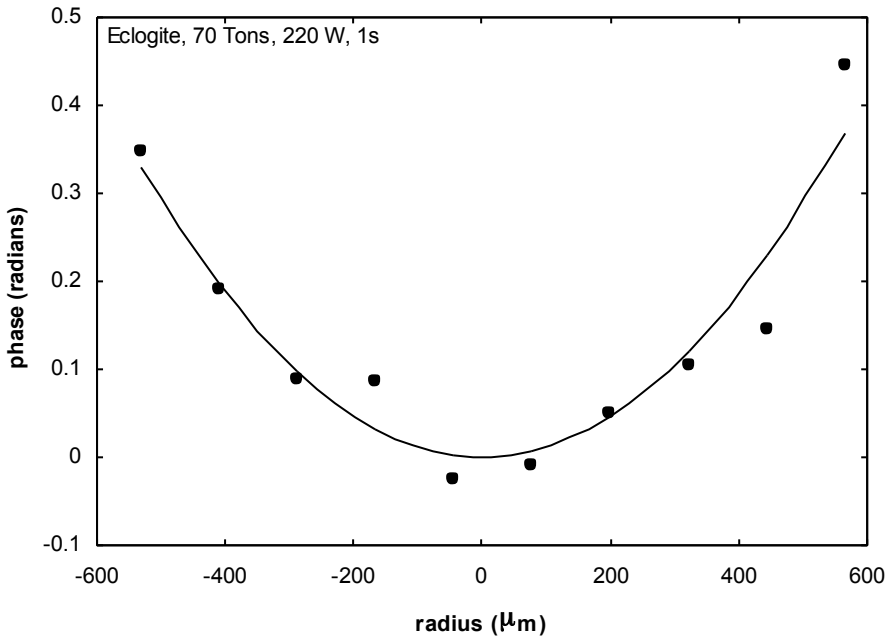
Eclogite, 70 Tons, 220 W, 1s
phase (radians)
radius (μm)
0.5
0.4
0.3
0.2
0.1
0
-0.1
-600
-400
-200
0
200
400
600

Figure 3

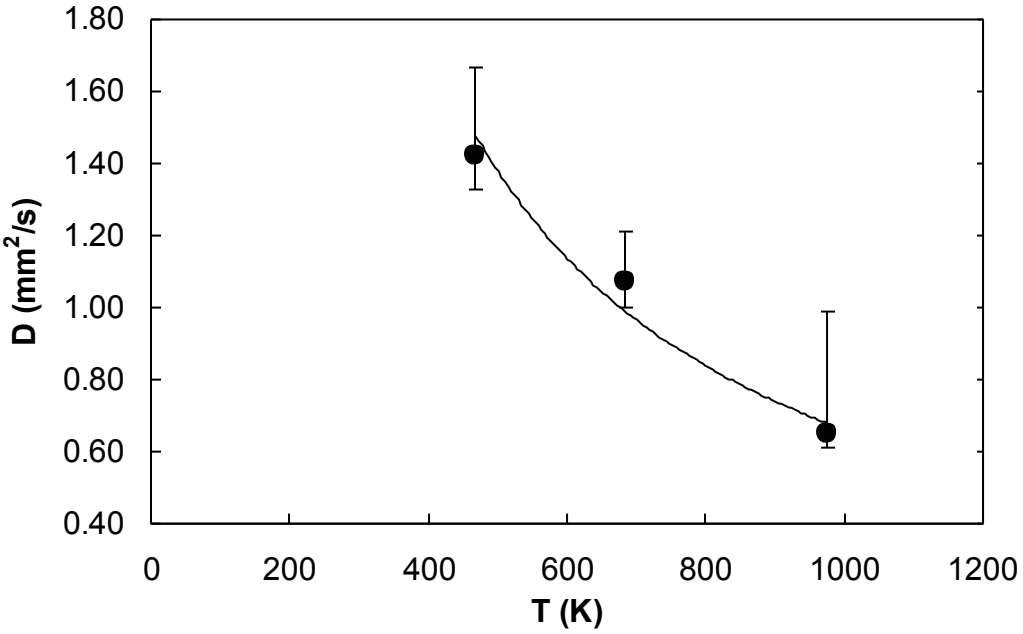
1.80
1.60
1.40
1.20
1.00
0.80
0.60
0.40
D (mm²/s)
0
200
400
600
800
1000
1200
T (K)

Figure 4.

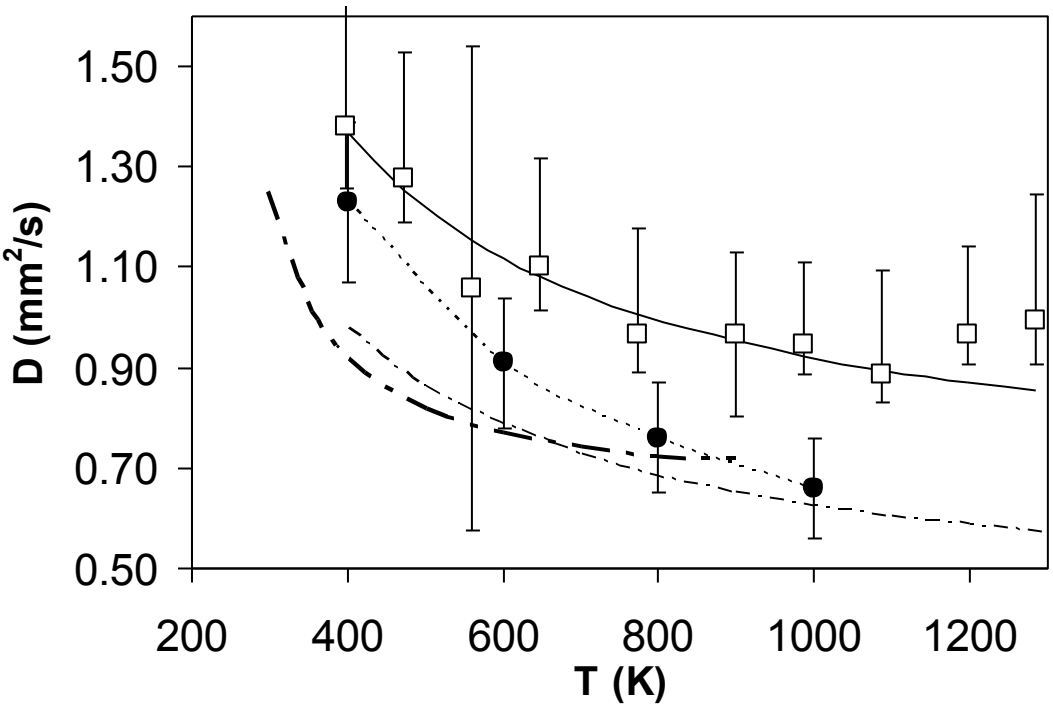

Figure 5

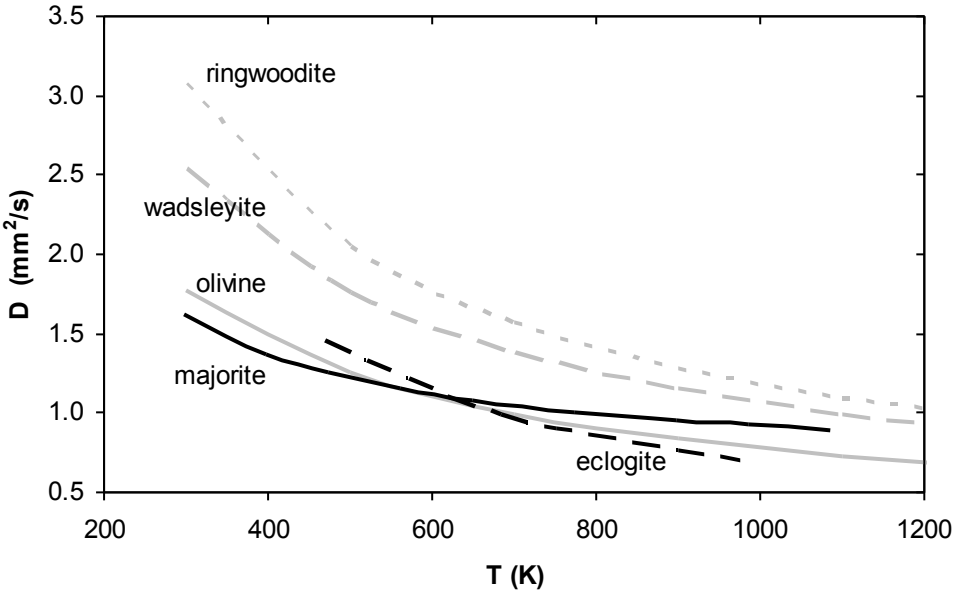
3.5
3.0
2.5
2.0
1.5
1.0
0.5
D (mm²/s)
200
400
600
800
1000
1200
T (K)
ringwoodite
wadsleyite
olivine
majorite
eclogite

Figure 6

Table 1.

Bulk composition of the MORB glass starting material in atomic percent.

SiO_2	50.12
TiO_2	1.14
Al_2O_3	15.04
FeO	9.06
MnO	0.15
MgO	9.62
CaO	11.8
Na_2O	2
K_2O	0.22
P_2O_5	0.12